EFFECTS OF ELECTROMAGNETIC FIELD ON THE THERMAL PERFORMANCE OF LONGITUDINAL POROUS FINS WITH TEMPERATURE-DEPENDENT INTERNAL HEAT GENERATION

Adesola Oluwatomi Osikoya[1], *Gbeminiyi Musibau Sobamowo*[2,*], *Suraju Aremu Oladosu* [1]

[1]Department of Mechanical Engineering, Lagos State University, Epe, Lagos, Nigeria.
[2]Department of Mechanical Engineering, University of Lagos, Akoka, Lagos, Nigeria.

*Corresponding Author: Gbeminiyi Musibau Sobamowo (Email: mikegbeminiyiprof@yahoo.com)
(Received: 08-October-2024; accepted: 21-July-2025; published: 30-September-2025)
http://dx.doi.org/10.55579/jaec.202593.469

Abstract. *Excessive heat generation in systems often leads to their thermally-induced failures, continuous technical progress is important for high-performance equipment. Therefore, there is a need for an effective cooling of the such thermal equipment. In this present work, the thermal behavior of a convective rectangular porous fin exposed to an electric and magnetic field and with temperature-dependent internal heat generation was studied using differential transformation method. A good agreement was established between the results of the differential transformation method and the numerical method's results. Consequently, the significance of electromagnetic, porosity, convective, internal heat generation on the thermal performance of the porous fin are investigated using the approximate analytical method. The exploration of the impacts of the parameters on the passive device reveals that increasing the electromagnetic field, porosity and convective heat transfer parameters cause increase in the rate of heat transfer from the base of the fin. However, an increase in the internal heat generation and the thermal conductivity parameters cause the fin temperature to increase. It is believed that the present work will help in the better design of the passive device especially in an electromagnetic environment.*

Keywords: *Electromagnetic Field; Porous Fin; Heat transfer, Internal heat generation; Differential Transformation Method.*

1. Introduction

Advancements in technology are always needed for high-performance systems, yet excessive heat generation can lead to thermally-induced failure in these systems. Therefore, the thermal equipment of this kind needs to be effectively cooled. Numerous practical and theoretical studies have been prompted by this requirement. Such studies are developed for evaluating the thermal performance of porous fins in natural convection situations as a result of the pioneer work of Kiwan and Al-Nimr [1]. Further studies have been presented by some researchers on the study of porous fins in thermal systems, electronic components, and sensitive devices (Kiwan [2–4], Gorla and Bakier

[5], Kundu and Bhanja [6], Kundu et al. [7], Taklifi et al. [8], Bhanja and Kundu [9] and Kundu et al. [10], Gorla et al. [11], Moradi et al. [12], Ha et al. [13], Hoshyar et al. [14], Hatami and Ganji [15, 16], Rostamiyaan et al. [17], and Ghasemi et al. [18]). These researchers employed a variety of mathematical methods for assessing the thermal response porous fins in conditions of natural convection. The approximate analytical techniques adopted include variational iterative method (VIM), Adomian Decomposition method (ADM), Spectral Collocation, Homotopoy Perturbation method (HPM), Homotopy Analysis method (HAM0), and Differential Transformation method (DTM). Also, with the aid of various approximate analytical and numerical techniques, Oguntala et al. [19–28] and Sobamowo et al. [3, 28–30] have studied extensively on porous fins under convective-radiative heat transfer and magnetic field.

The above review works applied some approximate analytical methods. However, these methods have inherent limitations. It has been stated that the HPM is limited to weakly nonlinear problems while ADM poses some challenges in the determination of Adomian polynomials. The lack of rigorous theories or appropriate guidance for selecting initial approximation, auxiliary linear operators, auxiliary functions, and auxiliary parameters limits the use of HAM [29–33]. Furthermore, reviewed research indicates that the differential transformation method's use has been restricted to the thermal analysis of solid fins in non-magnetic environments. Zhou first proposed the differential transform method (DTM), which has since gained popularity and been used in several engineering and scientific research publications to handle nonlinear issues due to relative benefits over other approximate analytical techniques. This method works without linearization, discretization, restricted assumptions, perturbation, or discretization round-off error. It solves nonlinear integral and differential equations very efficiently. It lessens the computing challenges as compared to the other conventional methods as well. A closed form series solution or an approximate solution can be produced with DTM since it offers highly accurate and good approximations to the solution of non-linear equations. It can provide the series solution with a quick convergence rate and accuracy while drastically lowering the amount of computational work, cost and time. When compared to other approximative analytical or numerical methods, this approach is more practical for engineering computations because of its ability to lower calculation costs, it seems more enticing than the numerical solution in solving nonlinear problems. Therefore, this paper utilized differential transformation method to analyzed the thermal behavior of a convective-radiative porous fin under the influence of electromagnetic fields with temperature-dependent internal heat generation. With the aid of the thermal model solution, the effects of electromagnetic fields, internal heat generation, radiative and convective heat transfer on the porous fins are analyzed, presented and discussed.

2. Problem formulation

Examine a convective-radiative porous fin with length L and thickness t that is subjected to a magnetic field and exposed on both faces to a convective environment at a specific temperature, as illustrated in Figure 1. In order to facilitate the problem analysis, the following presumptions are made.

1. The fluid in the porous medium is homogeneous, isotropic, and saturated with a single-phase fluid.
2. Both solid and fluid physical properties are taken as constants, with the exception of the liquid density, which could have an impact on the buoyancy term when the Boussinesq approximation that is employed.
3. In the domain, porous and fluid media are in a locally thermodynamic equilibrium.
4. Radiative transfers, surface convection, and non-Darcian effects are neglected.
5. The temperature varies steadily only one-dimensional,
6. The fin tip is of the adiabatic type, and the fin base has no thermal contact resistance.

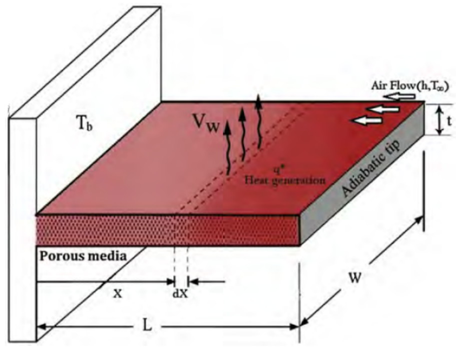

Fig. 1: Schematic of the convective-radiative longitudinal porous fin.

The thermal energy balance may be represented in accordance with the previously given assumptions and Darcy's model (Oguntala et al., [19, 20, 27, 28]; Sobamowo et al., [29–33]).

$$q_x - \left(q_x + \frac{\delta q}{\delta x}dx\right) + q\left(T\right)dx = \dot{m}c_p(T - T_a) + hP(1-\widetilde{\varepsilon})(T - T_a)dx + \sigma\varepsilon P(T^4 - T_a^4)dx + \delta_b\zeta E^2 dx + \frac{\mathbf{J}_c \times \mathbf{J_c}}{\sigma}dx \tag{1}$$

where

$$\mathbf{J_c} = \sigma\left(\mathbf{E} + \mathbf{V} \times \mathbf{B}\right) \tag{2}$$

The mass flow rate of the fluid through the porous material is given as

$$\dot{m} = \rho u(x) W dx \tag{3}$$

Adopting the Darcy's Model

$$u(x) = \frac{gK\beta}{v}\left(T - T_a\right) \tag{4}$$

Then, Eq. (1) becomes

$$q_x - \left(q_x + \frac{\delta q}{\delta x}dx\right) + q\left(T\right)dx = \frac{\rho c_p gK\beta}{v}(T - T_a)^2 dx + hP(1-\widetilde{\varepsilon})(T - T_a)dx + \sigma\varepsilon P(T^4 - T_a^4)dx + \delta_b\zeta E^2 dx + \frac{\mathbf{J_c} \times \mathbf{J_c}}{\sigma}dx \tag{5}$$

As $dx \to 0$, Eq. (5) reduces

$$-\frac{dq}{dx} + q\left(T\right) = \frac{\rho c_p gK\beta}{v}(T - T_a)^2 + hP(1-\widetilde{\varepsilon})(T - T_a) + \sigma\varepsilon P(T^4 - T_a^4) + \delta_b\zeta E^2 + \frac{\mathbf{J_c} \times \mathbf{J_c}}{\sigma} \tag{6}$$

Using Fourier's law of heat conduction, the rate of heat conduction in the fin is given by

$$q = -k_{eff}A_{cr}\frac{dT}{dx} \tag{7}$$

where

$$k_{eff} = \phi k_f + (1-\phi)k_s$$

Based on Rosseland diffusion approximation, the radiation heat transfer rate is

$$q = -\frac{4\sigma A_{cr}}{3\beta_R}\frac{dT^4}{dx} \tag{8}$$

$$q = -k_{eff}A_{cr}\frac{dT}{dx} - \frac{4\sigma A_{cr}}{3\beta_R}\frac{dT^4}{dx} \tag{9}$$

The substitution of Eq. (9) into Eq. (6), provides

$$\frac{d}{dx}\left(k_{eff}A_{cr}\frac{dT}{dx} + \frac{4\sigma A_{cr}}{3\beta_R}\frac{dT^4}{dx}\right) + q\left(T\right) = \frac{\rho c_p gK\beta}{v}(T - T_a)^2 + hP(1-\widetilde{\varepsilon})(T - T_a) + \sigma\varepsilon P(T^4 - T_a^4) + \delta_b\zeta E^2 + \frac{\mathbf{J_c} \times \mathbf{J_c}}{\sigma} \tag{10}$$

Further simplification of Eq. (10) gives the governing differential equation for the fin as

$$\frac{d^2T}{dx^2} + \frac{4\sigma}{3\beta_R k_{eff}}\frac{d}{dx}\left(\frac{dT^4}{dx}\right) - \frac{\rho c_p gK\beta}{k_{eff}tv}(T - T_a)^2 - \frac{h(1-\widetilde{\varepsilon})}{k_{eff}t}(T - T_a) - \frac{\sigma\varepsilon}{k_{eff}t}(T^4 - T_a^4) - \frac{\delta_b\zeta E^2}{k_{eff}A_{cr}} - \frac{\mathbf{J_c} \times \mathbf{J_c}}{\sigma k_{eff}A_{cr}} + \frac{q\left(T\right)}{k_{eff}A_{cr}} = 0 \tag{11}$$

The boundary conditions are

$$\begin{array}{ll} x = 0, & \frac{dT}{dx} = 0 \\ x = L, & T = T_b \end{array} \tag{12}$$

But

$$\frac{\mathbf{J_c} \times \mathbf{J_c}}{\sigma} = \sigma B_o^2 u^2 \tag{13}$$

After substitution of Eq. (13) into Eq. (11),

$$\frac{d^2T}{dx^2} + \frac{4\sigma}{3\beta_R k_{eff}}\frac{d}{dx}\left(\frac{dT^4}{dx}\right) - \frac{\rho c_p gK\beta}{k_{eff}tv}(T - T_a)^2 - \frac{h(1-\widetilde{\varepsilon})}{k_{eff}t}(T - T_a) - \frac{\sigma\varepsilon(T^4 - T_a^4)}{k_{eff}t} - \frac{\delta_b\zeta E^2}{k_{eff}A_{cr}} - \frac{\sigma B_o^2 u^2}{k_{eff}A_{cr}} + \frac{q\left(T\right)}{k_{eff}A_{cr}} = 0 \tag{14}$$

In this paper, a situation where there is a small temperature differential within the material is taken into account. Actually, this meant that the temperature-invariant thermal and physical properties of the fin had to be used. Moreover, the term T^4 in this instance has been demonstrated to be a linear function of temperature. As such, we have

$$T^4 = T_\infty^4 + 4T_\infty^3 (T - T_\infty) + 6T_\infty^2 (T - T_\infty)^2 + ... \cong 4T_\infty^3 T - 3T_\infty^4 \quad (15)$$

Given that

$$q(T) = q_0 [1 + \lambda (T - T_\infty)]$$

when Eq. (15) is substituted into Eq. (14), then

$$\frac{d^2T}{dx^2} + \frac{16\sigma}{3\beta_R k_{eff}} \frac{d^2T}{dx^2} - \frac{\rho c_p g K \beta}{k_{eff} t v}(T - T_a)^2 - \frac{h(1-\tilde{\varepsilon})}{k_{eff} t}(T - T_a) - \frac{4\sigma\varepsilon T_a^3 (T - T_a)}{k_{eff} t} - \frac{\sigma B_o^2 u^2}{k_{eff} A_{cr}} - \frac{\delta_b \zeta E^2}{k_{eff} A_{cr}} + \frac{q_o}{k_{eff} A_{cr}} [1 + \lambda (T - T_\infty)] = 0 \quad (16)$$

Using following dimensionless parameters in Eq. (15) into Eq. (16),

$$X = \frac{x}{L}, \quad \theta = \frac{T - T_a}{T_b - T_a}, \quad Ra = Gr.Pr = \left(\frac{\beta' g T_b t^3}{\nu_f^2}\right)\left(\frac{\rho c_p \nu_f}{k_{eff,a}}\right),$$
$$Rd = \frac{4\sigma_{st} T_\infty^3}{3\beta_R k_{eff}}, H_m = \frac{\sigma B_0^2 u^2 L^2}{k_{eff} A_{cr} (T_b - T_a)}$$
$$Da = \frac{K}{t^2}, \quad Q = \frac{q_o}{k_{eff} A_{cr} (T_b - T_a)}, \quad M^2 = \frac{h(1-\tilde{\varepsilon})L^2}{k_{eff,a} t},$$
$$Nr = \frac{4\sigma_{st} T_a^3 L^2}{k_{eff,a} t}, \quad E_b = \frac{\delta_b \zeta E^2 L^2}{k_{eff} A_{cr} (T_b - T_a)},$$
$$S_h = \left(\frac{\beta' g (T_b - T_a) t^3}{\nu_f^2}\right)\left(\frac{\rho c_p \nu_f K}{k_{eff,a} t^2}\right)\frac{(L/t)^2}{k_{eff,a}} = \frac{RaDa(L/t)^2}{k_{eff,a}}$$
$$\gamma = \lambda (T_b - T_a) \quad (17)$$

we arrived at the dimensionless form of the governing Eq. (16) as

$$(1 + 4Rd) \frac{d^2\theta}{dX^2} - Ra\theta^2 - M^2\theta - Nr\theta - H_m - E_b + Q(1 + \gamma\theta) = 0 \quad (18)$$

Or

$$\frac{d^2\theta}{dX^2} - \frac{Ra}{(1+4Rd)}\theta^2 - \frac{Nc(1-\tilde{\varepsilon})}{(1+4Rd)}\theta - \frac{Nr}{(1+4Rd)}\theta - \frac{H_m}{(1+4Rd)} - \frac{E_b}{(1+4Rd)} + \frac{Q}{(1+4Rd)}(1 + \gamma\theta) = 0 \quad (19)$$

Which can be written as

$$\frac{d^2\theta}{dX^2} - S_h\theta^2 - M_a^2\theta - H + G(1 + \gamma\theta) = 0 \quad (20)$$

where

$$S_h = \frac{Ra}{(1+4Rd)}, M^2 = \frac{Nc(1-\tilde{\varepsilon})}{(1+4Rd)} + \frac{Nr}{(1+4Rd)},$$
$$G = \frac{Q}{(1+4Rd)}, E_H = \frac{H_m + E_b}{(1+4Rd)},$$

The dimensionless boundary conditions

$$X = 0, \quad \theta = 1, \qquad X = 1, \quad \frac{d\theta}{dX} = 0, \quad (21)$$

3. Method of Solution: Differential Transform Method

The nonlinearities in Eqs. (20) and (21) call for the use of an approximate analytical method or a numerical method. In this study, we use differential transformation method. The definition and the operational properties of the method can be found in our previous study [25].

If $u(t)$ is analytic in the domain T, then it will be differentiated continuously with respect to time t.

$$\frac{d^p u(t)}{dt^p} = \varphi(t, p) \text{ for all } t \in T \quad (22)$$

for $t = t_i$, then $\varphi(t, p) = \varphi(t_i, p)$, where p belongs to the set of non-negative integers, denoted as the p-domain. Therefore Eq. (22) can be rewritten as

$$U(p) = \varphi(t_i, p) = \left[\frac{d^p u(t)}{dt^p}\right]_{t=t_i} \quad (23)$$

where U_p is called the spectrum of $u(t)$ at $t = t_i$ If $u(t)$ can be expressed by Taylor's series, the $u(t)$ can be represented as

$$u(t) = \sum_p^\infty \left[\frac{(t - t_i)^p}{p!}\right] U(p) \quad (24)$$

Where Equ. (24) is called the inverse of using the symbol 'D' denoting the differential transformation process and combining (23) and (24), it is obtained that

$$u(t) = \sum_{p=0}^\infty \left[\frac{(t - t_i)^p}{p!}\right] U(p) = D^{-1}U(p) \quad (25)$$

3.1. Operational properties of differential transformation method

If $u(t)$ and $v(t)$ are two independent functions with time (t) where $U(p)$ and $V(P)$ are the transformed function corresponding to $u(t)$ and $v(t)$, then it can be proved from the fundamental mathematics operations performed by differential transformation that.

1. If $z(t) = u(t) \pm v(t)$, then $Z(p) = U(p) \pm V(p)$
2. If $z(t) = \alpha u(t)$, then $Z(p) = \alpha U(p)$
3. If $z(t) = \frac{du(t)}{dt}$, then $Z(p) = (p-1)U(p+1)$
4. If $z(t) = u(t)v(t)$, then $Z(p) = \sum_{r=0}^{p} V(r)U(p-r)$
5. If $z(t) = u^m(t)$, then $Z(p) = \sum_{r=0}^{p} U^{m-1}(r)U(p-r)$
6. If $z(t) = u(t)v(t)$, then $Z(k) = \sum_{r=0}^{p} (r+1)V(r+1)U(p-r)$

$\frac{d^2\theta}{dX^2} - S_h\theta^2 - M_a^2\theta - E_H + G(1+\gamma\theta) = 0$

The differential transformation of the Eq. (20) are given as

$$(p+1)(p+2)\theta(p+2) - M^2\theta(p) - S_h \sum_{r=0}^{p} \theta(r)\theta(p-r) + G\gamma\theta(p) + (G - E_H)\delta(p) = 0 \tag{26}$$

where

$$\theta(p+2) = \frac{M^2\theta(p) + S_h \sum\limits_{r=0}^{p} \theta(r)\theta(p-r) - G\gamma\theta(p) - (G-E_H)\delta(p)}{(p+1)(p+2)} \tag{27}$$

With the boundary conditions,

$$\theta(0) = 1, \quad \theta(1) = a,$$

We arrived at

$$\begin{aligned}
\theta(2) &= \frac{-(G-E_H)}{2} + \frac{aS_h}{2} + \frac{M^2}{2} - \frac{G\gamma}{2} \\
\theta(3) &= \frac{aS_h}{3} + \frac{M^2 a}{6} - \frac{aG\gamma}{6} \\
\theta(4) &= \frac{-S_h G\gamma}{8} - \frac{S_h(G-E_H)}{12} + \frac{S_h^2}{12} + \frac{S_h M^2}{8} - \frac{M^2 G\gamma}{12} \\
&\quad + \frac{a^2 S_h^2}{12} - \frac{M^2(G-E_H)}{24} + \frac{M^4}{24} + \frac{M^2 G^2\gamma}{24} + \frac{M^2 G^2\gamma^2}{24} \\
\theta(5) &= \frac{-S_h a(G-E_H)}{20} - \frac{S_h^2 a}{12} + \frac{S_h a M^2}{12} - \frac{S_h a G\gamma}{12} + \frac{aM^4}{120} \\
&\quad - \frac{aM^2 G\gamma}{60} + \frac{M^2 a G^2}{120}
\end{aligned} \tag{28}$$

Therefore, from the definition

$$\begin{aligned}
\theta(X) = 1 + aX &+ \left(\frac{aS_h}{2} - \frac{(G-H)}{2} + \frac{M^2}{2} - \frac{G\gamma}{2}\right)X^2 + \left(\frac{aS_h}{3} + \frac{M^2 a}{6} - \frac{aG\gamma}{6}\right)X^3 \\
&+ \left(\begin{matrix} \frac{S_h M^2}{8} - \frac{S_h G\gamma}{8} - \frac{S_h(G-H)}{12} + \frac{S_h^2}{12} - \frac{M^2 G\gamma}{12} + \frac{aS_h^2}{12} \\ -\frac{M^2(G-H)}{24} + \frac{M^4}{24} + \frac{M^2 G^2\gamma}{24} + \frac{M^2 G\gamma^2}{24} \end{matrix}\right)X^4 \\
&+ \left(\begin{matrix} \frac{S_h^2 a M^2}{12} - \frac{S_h a(G-H)}{20} - \frac{S_h^2 a}{12} - \frac{S_h a G\gamma}{12} \\ +\frac{aM^4}{120} - \frac{aM^2 G\gamma}{60} + \frac{M^2 a G\gamma^2}{120} \end{matrix}\right)X^5 + \ldots.
\end{aligned} \tag{29}$$

In order to find 'a', we apply the end boundary condition $X = 1$, $\theta = 1$ which gives

$$\begin{aligned}
1 = 1 + a &+ \left(\frac{aS_h}{2} - \frac{(G-H)}{2} + \frac{M^2}{2} - \frac{G\gamma}{2}\right) + \left(\frac{aS_h}{3} + \frac{M^2 a}{6} - \frac{aG\gamma}{6}\right) \\
&+ \left(\begin{matrix} \frac{S_h M^2}{8} - \frac{S_h G\gamma}{8} - \frac{S_h(G-H)}{12} + \frac{S_h^2}{12} - \frac{M^2 G\gamma}{12} + \frac{aS_h^2}{12} \\ -\frac{M^2(G-H)}{24} + \frac{M^4}{24} + \frac{M^2 G^2\gamma}{24} + \frac{M^2 G\gamma^2}{24} \end{matrix}\right) \\
&+ \left(\begin{matrix} \frac{S_h^2 a M^2}{12} - \frac{S_h a(G-H)}{20} - \frac{S_h^2 a}{12} - \frac{S_h a G\gamma}{12} \\ +\frac{aM^4}{120} - \frac{aM^2 G\gamma}{60} + \frac{M^2 a G\gamma^2}{120} \end{matrix}\right) + \ldots.
\end{aligned} \tag{30}$$

4. Results and Discussion

MATLAB is used to code and simulate the developed solutions of the thermal model. However, prior to being utilized for parametric studies, the solutions of DTM f must first be verified. Consequently, in order to do this, the governing differential equation is numerically solved using the fourth-order Runge-Kutta method (4^{th} RKM). The outcomes of the 4^{th} RKM and DTM are shown, as Table 1 illustrates. According to the Table, the DTM is highly accurate and exhibits good agreement with the numerical method. This section presents the graphical representations of the outcomes using the developed models. Figure 2 shows how the temperature distribution in the porous fin is affected by porosity, or the porous parameter. As can be seen in the figures, the temperature in the fin

Tab. 1: Comparison of results.

X	4^{th} RKM	Present (DTM)
0.0	1.000000	1.000000
0.2	0.958709	0.958714
0.4	0.927017	0.927029
0.6	0.904595	0.904613
0.8	0.891243	0.891256
1.0	0.886794	0.886807

drops faster as the porosity parameter increases, and as the temperature reduces faster, the rate of heat transfer—that is, convective-radiative heat transfer—through the fin increases. The Raleigh number rises in tandem with the porosity parameter, increasing the porous fin's permeability and the working fluid's capacity to flow through its pores. As a result, the buoyancy force is increased, causing the fin to convect more heat and rapidly drop in temperature. The fin performs better thermally and has better heat transmission. Fin porosity rises with increased convective heat transfer, improving fin efficiency.

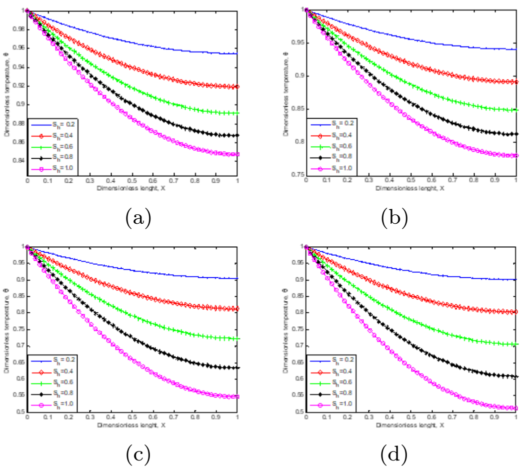

Fig. 2: Impacts of porosity on the fin temperature when (a) $M = 0.5, Q = 0.2, \gamma = 0.4$, (b) $M = 1, Q = 0.2, \gamma = 0.4$, (c) $M = 5, Q = 0.4, \gamma = 0.2$, (d) $M = 10, Q = 0.2, \gamma = 0.4$.

Figures 3a-d and 4a-b illustrate how the internal heat parameter affects the porous fin's thermal response. It is evident that the fin's thermal performance is reduced by the internal heat parameter. Furthermore, it is demonstrated that the fin retains heat instead of dissipating it, thus defeating the goal of heat dissipation by the porosity when the internal heat parameter rises to specific values.

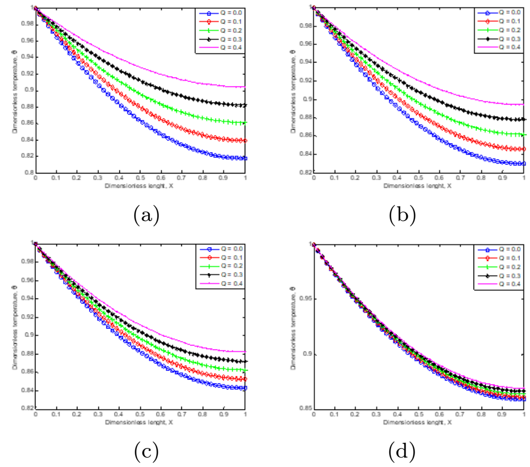

Fig. 3: Influences of internal heat parameter on the fin temperature distribution when (a) $M = 0.1, S_h = 0.5, \gamma = 0.2$, (b) $M = 0.5, S_h = 0.5, \gamma = 0.2$, (c) $M = 0.75, S_h = 5.0, \gamma = 0.2$, (d) $M = 1.0, S_h = 0.5, \gamma = 0.2$.

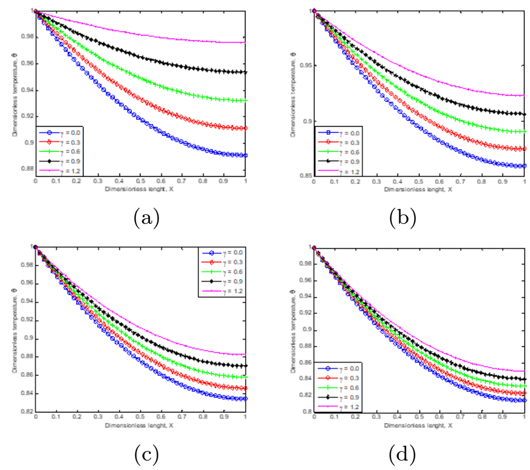

Fig. 4: Effects of the internal heat parameter on fin temperature when (a) $M = 0.1, Q = 0.4, S_h = 0.5$, (b) $M = 1.0, Q = 0.4, S_h = 0.5$, (c) $M = 1.5, Q = 0.4, S_h = 0.5$, (d) $M = 2.0, Q = 0.4, S_h = 0.5$.

While Figure 4 illustrates the impacts of a temperature-dependent internal heat production parameter on the temperature distribution in the fin, Figure 7 show the effects of an internal heat generation parameter on the temperature distribution in the porous fin. According to the figures, the temperature gradient of the fins diminishes as the internal heat generating parameters increase, which in turn causes a drop in the fin's rate of heat transmission. It should be noted that because of their low heat conductivity and high surface area when in contact with the cooling fluid, fins made of porous material function better and weigh far less than fins made of solid metal.

Figure 7 shows the effects of an internal heat generation parameter on the temperature distribution in the porous fin, whereas Figure 4 shows the effects of a temperature-dependent internal heat production parameter on the temperature distribution in the fin. The figures show that when the internal heat generating parameters increase, the fins' temperature gradient decreases, leading to a decrease in the fins' heat transmission rate. It should be mentioned that fins made of porous material perform better and weigh significantly less than fins made of solid metal due to their low heat conductivity and high surface area when in contact with the cooling fluid.

Figure 3 shows how the conduction-convection parameter affects the temperature distribution of the fin. The figure illustrates how the conduction-convection parameter grows with the rate of heat transfer through the fin. This is due to the fact that the fin becomes steeper and reflects higher base heat flow rates as its temperature drops more quickly. A profile with a smaller value of the conduction-convection term has the steepest temperature gradient. But because of its lower thermal conductivity compared to the values of Nc in the other profiles, which leads to a reduced heat-transfer rate, its value is noticeably higher. This indicates that while the objective (high effective use of the fin) is to minimize the convective parameter, the fin's thermal performance or efficiency is preferable at low convective parameter values. The optimal situation is $T = Tb$ everywhere, where there is a temperature drop throughout the fin length. It's crucial to remember that a small value for M denotes a thin, comparatively short fin with low thermal conductivity, while a high value for M denotes a lengthy, low thermal conductivity fin. Since the fin's thermal performance or efficiency is optimum at low convective fin parameter values, very long fins should be avoided in practice.

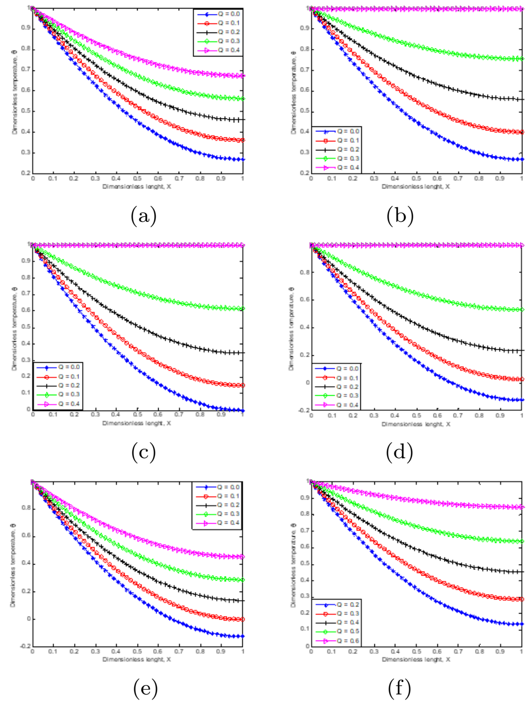

Fig. 5: Impacts of internal heat values on when (a) $S = 0, M = 2, G = 0.5$, (b) $S = 0, M = 2, G = 1.5$, (c) $S = 0, M = 3.35, G = 1.5$, (d) $S = 0, M = 5.0, G = 1.5$, (e) $S = 0, M = 5, G = 0.5$, (f) $S = 0, M = 5.0, G = 0.5$.

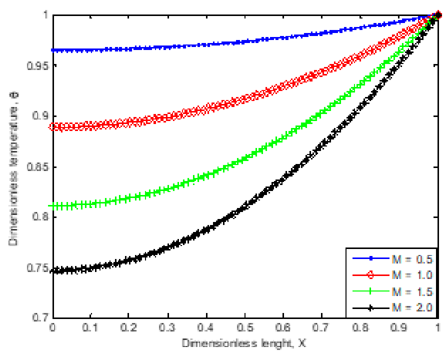

Fig. 6: Dimensionless temperature distribution in the fin parameters for varying convection-conduction parameter.

The effect of the conduction-radiation parameter is seen in Figure 4. The graph shows how increasing the conduction-radiation parameter

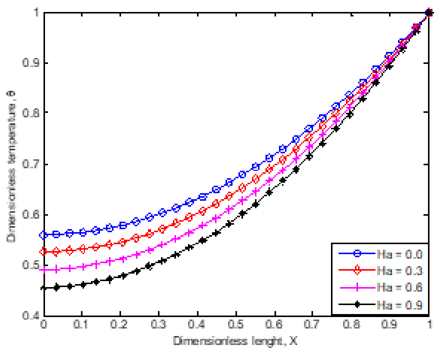

Fig. 7: Dimensionless temperature distribution in the fin parameters for varying magnetic parameter.

improves the rate of heat transfer through the fin. Figure 5 shows how the magnetic parameter, also known as the Hartman number, affects the temperature distribution in the porous fin. The graphic shows how the induced magnetic field within the fin might lead to improved heat transfer via porous fins. The effect of the electric field on the thermal performance of the fin showed the similar pattern. Thus, figures 2–6 show how improving the fin's porosity, convective, radiative, and magnetic properties increases the fin's efficiency by hastening heat transfer from the fin.

5. Conclusion

This work adopted the differential transformation method to assess the impacts of electromagnetic field on the thermal behavior of a convecting porous fin with temperature-dependent internal heat generation. Also, the significances of other controlling parameters on the thermal performance of the porous fin were examined using the established symbolic heat transfer models. It was found that increasing the electric field, magnetic field, porosity, convective heat transfer parameters cause increase in the rate of heat transfer from the base of the fin. However, an increase in the internal heat generation and the thermal conductivity parameters cause the fin temperature to increase. The work will help in the better design of the passive device especially in an electromagnetic environment.

Nomenclature

$\mathbf{J}$	conduction current intensity
A	cross sectional area of the fins
A_b	porous fin base area
A_s	porous fin surface area
B_0	magnetic field intensity
c_p	specific heat of the fluid passing through porous fin
Da	darcy number
E	electric field
g	gravity constant
h	heat transfer coefficient over the fin surface
h_b	heat transfer coefficient at the base of the fin
J_c	conduction current intensity
K	permeability of the porous fin
k	thermal conductivity of the fin material
k_b	thermal conductivity of the fin material at the base of the fin
k_r	thermal conductivity ratio
k_{eff}	effective thermal conductivity ratio
L	length of the fin, (m)
M	dimensionless thermo-geometric parameter
m	mass flow rate of fluid passing through porous fin
Nu	nusselt number
P	fin perimeter (m)
P	perimeter of the fin
Q	dimensionless heat transfer rate per unit area
q	internal heat generation

q_b heat transfer rate per unit area at the base

Q_s dimensionless heat transfer rate the base

R_2 surface-ambient radiation parameter

Ra Rayleigh number

$Ra*$ modified Rayleigh number

Rd radiation–conduction parameter

S_h porosity parameter

T fin temperature

t thickness of the fin

T_a ambient temperature

T_b temperature at the base of the fin

u axial velocity

v average velocity of fluid passing through

w width of the fin

X dimensionless length of the fin

x axial length measured from fin tip

Greek Symbols

α Thermal diffusivity

β_R Rosseland extinction coefficient

ε Emissivity

μ Dynamic viscosity

ν Kinematic viscosity

σ Electric conductivity

σ_{st} Stefan–Boltzmann constant

ρ Density of the fluid

ρ_ε Electrical density

References

[1] S. Kiwan and A. Al-Nimr. Using porous fins for heat transfer enhancement. *ASME J. Heat Transf.*, 123:790–795, 2001.

[2] S. Kiwan. Effect of radiative losses on the heat transfer from porous fins. *Int. J. Therm. Sci.*, 46:1046–1055, 2007.

[3] S. Kiwan. Thermal analysis of natural convection porous fins. *Transp. Porous Media*, 67:17–29, 2007.

[4] S. Kiwan and O. Zeitoun. Natural convection in a horizontal cylindrical annulus using porous fins. *Int. J. Numer. Methods for Heat Fluid Flow*, 18(5):618–634, 2008.

[5] R. S. Gorla and A. Y. Bakier. Thermal analysis of natural convection and radiation in porous fins. *Int. Commun. Heat Mass Transf.*, 38:638–645, 2011.

[6] B. Kundu and D. Bhanji. An analytical prediction for performance and optimum design analysis of porous fins. *Int. J. Refrig.*, 34:337–352, 2011.

[7] B. Kundu, D. Bhanja, and K. S. Lee. A model on the basis of analytics for computing maximum heat transfer in porous fins. *Int. J. Heat Mass Transf.*, 55(25-26):7611–7622, 2012.

[8] A. Taklifi, C. Aghanajafi, and H. Akrami. The effect of mhd on a porous fin attached to a vertical isothermal surface. *Transp. Porous Media*, 85:215–31, 2010.

[9] D. Bhanja and B. Kundu. Thermal analysis of a constructal t-shaped porous fin with radiation effects. *Int. J. Refrig.*, 34:1483–96, 2011.

[10] B. Kundu. Performance and optimization analysis of src profile fins subject to simultaneous heat and mass transfer. *Int. J. Heat Mass Transf.*, 50:1545–1558, 2007.

[11] R. Gorla, R.S. Darvishi, M. T. Khani, and F. Aziz. Effects of variable thermal conductivity on natural convection and radiation in porous fins. *Int. Commun. Heat Mass Transf.*, 38:638–645, 2013.

[12] A. Moradi, T. Hayat, and A. Alsaedi. Convective-radiative thermal analysis of triangular fins with temperature-dependent thermal conductivity by dtm. *Energy Convers. Manag.*, 77:70–77, 2014.

[13] H. Ha, D. D. Ganji, and M. Abbasi. Determination of temperature distribution for porous fin with temperature-dependent heat generation by homotopy analysis method. *J. Appl. Mech. And Eng.*, 4(1), 2005.

[14] H. A. Hoshyar, I. Rahimipetroudi, D. D. Ganji, and A. R. Majidian. Thermal performance of porous fins with temperature-dependent heat generation via homotopy perturbation method and collocation method. *J. Appl. Math. Comput. Mech.*, 14(4):53–65, 2015.

[15] M. Hatami and D. D. Ganji. Thermal performance of circular convective-radiative porous fins with different section shapes and materials. *Energy Convers. Manag.*, 76:185–193, 2013.

[16] M. Hatami and D. D. Ganji. Thermal behavior of longitudinal convective–radiative porous fins with different section shapes and ceramic materials (sic and si3n4). *Ceram. Int. journal*, 40:6765–6775, 2014.

[17] Y. Rostamiyan, D. D. Ganji, I. R. Petroudi, and M. K. Nejad. Analytical investigation of nonlinear model arising in heat transfer through the porous fin. *Therm. Sci.*, 18(2):409–417, 2014.

[18] S. E. Ghasemi, P. Valipour, M. Hatami, and D. D. Ganji. Heat transfer study on solid and porous convective fins with temperature-dependent heat - generation using efficient analytical method. *J. Cent. South Univ.*, 21:4592–4598, 2014.

[19] G. A. Oguntala, M. G. Sobamowo, and A. A. Yinusa. Transient analysis of functionally graded material porous fin under the effect of lorentz force using the integral transform method for improved electronic packaging. *Heat transfer*, pages 1–18, 2020.

[20] G. Oguntala, M. G. Sobamowo, R. Abd-Alhameed, and S. Jones. Efficient iterative method for the investigation of convective-radiative porous fin with internal heat generation under a uniform magnetic field. *Int. J. Appl. computational mathematics*, 5(1):1–9, 2019.

[21] G. Oguntala, M. G. Sobamowo, and R. Abd-Alhameed. Numerical analysis of transient response of convective-radiative cooling fin with convective tip under magnetic field for reliable thermal management of electronic systems. *Therm. Sci. Eng. Prog.*, 9:289–298, 2019.

[22] G. Oguntala, M. G. Sobamowo, R. Abd-Alhameed, and J. Noras. Numerical study of performance of porous fin heat sink of functionally graded material for improved thermal management of consumer electronics. *IEEE Trans. on Components, Packag. Manuf. Technol.*, PP(99):1271–1283, 2019.

[23] G. Oguntala, M. G. Sobamowo, R. Abd-Alhameed, and J. Noras. Investigation of simultaneous effects of surface roughness, porosity and magnetic field of rough porous micro-fin under a convective-radiative heat transfer for improved electronic cooling of microprocessors. *IEEE Trans. on Components, Packag. Manuf. Technol.*, 9(2):235–246, 2019.

[24] G. A. Oguntala, I. Danjuma, M. G. Sobamowo, R. Abd-Alhameed, and J. Noras. Nonlinear thermal analysis of a convective-radiative longitudinal porous fin of functionally graded material for efficient cooling of consumer electronics. *Int. J. Ambient Energy*, 2019.

[25] G. A. Oguntala, R. Abd-Alhameed, and M. G. Sobamowo. On the effect of magnetic field on thermal performance of convective-radiative fin with temperature-dependent thermal conductivity. *Karbala Int. J. Mod. Sci.*, 4:1–11, 2019.

[26] G. A. Oguntala, M. G. Sobamowo, A. A. Yinusa, and R. Abd-Alhameed. Application of approximate analytical technique using the homotopy perturbation method to

study the inclination effect on the thermal behavior of porous fin heat sink. *Math. Comput. Appl.*, 23(4):1–12, 2019.

[27] G. A. Oguntala, R. Abd-Alhameed, M. G. Sobamowo, and I. Danjuma. Performance, thermal stability and optimum design analyses of rectangular fin with temperature-dependent thermal properties and internal heat generation. *J. Comput. Appl. Mech.*, 49(1):37–43, 2019.

[28] G. A. Oguntala and M. G. Sobamowo. Galerkin's method of weighted residual for a convective straight fin with temperature-dependent conductivity and internal heat generation. *Int. J. Eng. Technol.*, 6(12):433–442, 2016.

[29] M. G. Sobamowo, G. Oguntala, and A. A. Yinusa. Nonlinear transient thermal modeling and analysis of a convective-radiative fin with functionally graded material in a magnetic environment. *Model. Simul. Eng.*, Article ID 7878564:16 pages, 2019.

[30] M. G. Sobamowo. Thermal analysis of longitudinal fin with temperature-dependent properties and internal heat generation using galerkin's method of weighted residual. *Appl. Therm. Eng.*, 99:1316–1330, 2016.

[31] M. G. Sobamowo, O. A. Adeleye, and A. A. Yinusa. Analysis of convective-radiative porous fin with temperature-dependent internal heat generation and magnetic using homotopy perturbation method. *J. computational Appl. Mech.*, 12(2):127–145, 2019.

[32] M.G. Sobamowo, O.M. Kamiyo, and O.A. Adeleye. Thermal performance analysis of a natural convection porous fin with temperature-dependent thermal conductivity and internal heat generation. *Therm. Sci. Eng. Prog.*, 1:39–52, 2017.

[33] M.G. Sobamowo. Singular perturbation and differential transform methods to two-dimensional flow of nanofluid in a porous channel with expanding/contracting walls subjected to a uniform transverse magnetic field. *Therm. Sci. Eng. Prog.*, 4:71–84, 2017.

About Authors

